

Integrating AI and Remote Sensing for Monitoring War-Impacted Agricultural Lands: Damage Assessment and Remediation Tracking

Sofia Drozd^{1,2,*†}, Andrii Shelestov^{1,2,†} and Nataliia Kussul^{1,2,3,†}

¹*National Technical University of Ukraine "Igor Sikorsky Kyiv Polytechnic Institute", 37, Prospect Beresteiskyi, Kyiv, 03056, Ukraine*

²*Space Research Institute National Academy of Sciences of Ukraine and State Space Agency of Ukraine, Glushkov Ave 40, 4/1, 03187, Kyiv, Ukraine*

³*University of Maryland, 2181 Samuel J. LeFrak Hall, 7251 Preinkert Drive, College Park, Maryland, 20742, USA*

Abstract

This paper presents the use of artificial intelligence (AI) and satellite data for monitoring the impacts of warfare on Ukraine's agricultural lands and tracking remediation measures implemented by organizations such as the HALO Trust.

The study highlights the use of AI-driven land cover classification maps for identification of damaged crop types and detection of field abandonment periods, as well as machine learning and deep learning techniques for automated recognition of damaged fields and crater mapping from high-resolution satellite imagery.

We conduct a comparative analysis of vegetation indices (NDVI) before and after remediation efforts across major crop types. Results reveal that even after comprehensive demining, war-damaged fields often remain uncultivated for 2-3 years and show 10–20% lower NDVI values than undamaged areas, particularly for sunflower and soybean crops. This persistent productivity gap underscores the need for long-term recovery strategies beyond initial remediation.

Additionally, soil erosion risk is evaluated using the RUSLE model, demonstrating that war damage increases erosion susceptibility across eastern Ukraine.

Overall, the research results show that AI greatly enhances satellite-based monitoring by enabling precise damage detection, remediation tracking, and predictive assessment of agricultural recovery. Its integration is essential for developing effective, scalable, and sustainable strategies to restore war-affected farmlands.

Keywords

AI, Machine learning, Neural networks, Crop classification, RUSLE, Satellite data, Field damage detection, Vegetation, Soil erosion, Remediation Measures

1. Introduction

The Russian invasion of Ukraine has had a profound impact on agricultural production for more than three years, affecting both domestic markets and export volumes [1]. Despite the devastation, Ukraine remains one of the world's major exporters of cereals and oilseeds [2], particularly to food-insecure regions in the Middle East and Africa. Yet, over three years since the start of the full-scale aggression on February 24, 2022, the consequences for global food security remain severe. Reduced cultivated areas, damaged and contaminated soils [3], and declining yields have cut Ukraine's exports to a fraction of pre-war levels, contributing to sharp increases in global food prices. The most acute impacts – land destruction, soil contamination [4], and abandonment – have occurred in recent growing seasons [5], undermining both immediate and long-term productivity.

In response, there is an urgent need for robust monitoring and evaluation systems to assess the effectiveness of remediation measures and to guide recovery strategies [6, 7]. Within the collaboration between the HALO Trust [8] and the KSE Agrocenter [9], a key priority is the development of a

ProfIT AI'25: 5th International Workshop of IT-professionals on Artificial Intelligence, October 15–17, 2025, Liverpool, UK

*Corresponding author.

†These authors contributed equally.

✉ sofi.drozd.13@gmail.com (S. Drozd); andrii.shelestov@gmail.com (A. Shelestov); kussul@umd.edu (N. Kussul)

>ID 0000-0002-5149-5520 (S. Drozd); 0000-0001-9256-4097 (A. Shelestov); 0000-0002-9704-9702 (N. Kussul)



© 2025 Copyright for this paper by its authors. Use permitted under Creative Commons License Attribution 4.0 International (CC BY 4.0).

systematic approach for monitoring conflict-affected farmland and evaluating the outcomes of soil remediation efforts. Traditional approaches relying on field surveys alone are insufficient, as they are costly, time-consuming, and often unsafe in war-affected zones.

Artificial intelligence (AI), combined with satellite-based remote sensing, provides an effective alternative [10]. AI-driven algorithms can process vast volumes of multispectral and ultra-high-resolution imagery, enabling rapid and scalable identification of crop types [11, 12, 13], periods of land abandonment [9, 14, 15], craters [16, 17, 18], and other damage indicators [19, 20, 21]. Moreover, AI enhances the interpretation of vegetation indices (such as NDVI) and supports predictive assessments of crop recovery and yield potential [22] after demining and remediation [23]. These capabilities allow for continuous, objective, and scalable monitoring at both local and national levels, directly supporting evidence-based recovery planning.

The aim of this study is to review and systematize AI- and satellite-based approaches for monitoring Ukraine's war-affected agricultural lands and for evaluating the effectiveness of remediation measures implemented by the HALO Trust. Specifically, the paper summarizes methods for identifying damaged crops and periods of land abandonment, mapping field damage and craters, and assessing erosion risks. We also analyze vegetation index dynamics and estimate potential yields on damaged fields before and after remediation, comparing them with pre-war periods and unaffected fields. The proposed approach demonstrates the potential of AI as a key instrument for building long-term monitoring systems and supporting decision-making for the recovery of Ukraine's agricultural sector.

2. Application of Machine Learning and Satellite Data for Monitoring Crop Types in Damaged Areas

To identify crop types that have been impacted by military activity, it is appropriate to use land cover classification maps generated from satellite imagery.

Since 2016, annual land cover maps with a spatial resolution of 10 meters have been available for Ukraine. These maps are produced in a cloud-based environment using data from Sentinel-1 and Sentinel-2 satellites, along with training datasets collected during annual field surveys conducted across various regions of Ukraine [11, 24].

The classification comprises 22 land cover classes, 13 of which represent specific agricultural crop types (see Table 1, where agricultural crops are underlined).

Table 1
Land cover classification map classes

Class ID	Class Label	Class ID	Class Label
1	Artificial	12	Bare land
2	<u>Wheat</u>	13	Water
3	<u>Rapeseed</u>	14	Wetland
4	<u>Buckwheat</u>	15	<u>Barley</u>
5	<u>Maize</u>	16	<u>Peas</u>
6	<u>Sugar beet</u>	17	<u>Alfalfa</u>
7	<u>Sunflower</u>	18	Gardens, parks
8	<u>Soybeans</u>	19	<u>Grape</u>
9	<u>Other crops</u>	20	Not cultivated
10	Forest	21	<u>Potato</u>
11	Grassland	23	Damaged Forest

Figure 1 shows an example of a land cover classification map for the year 2024, while Table 2 provides information on the classification accuracy for each class for 2016-2024 [24].

These maps can be used within any GIS platforms to determine the crop type that was present on a damaged field. The task involves extracting pixel values from the raster classification map within the boundaries of vector polygons outlining the damaged areas.

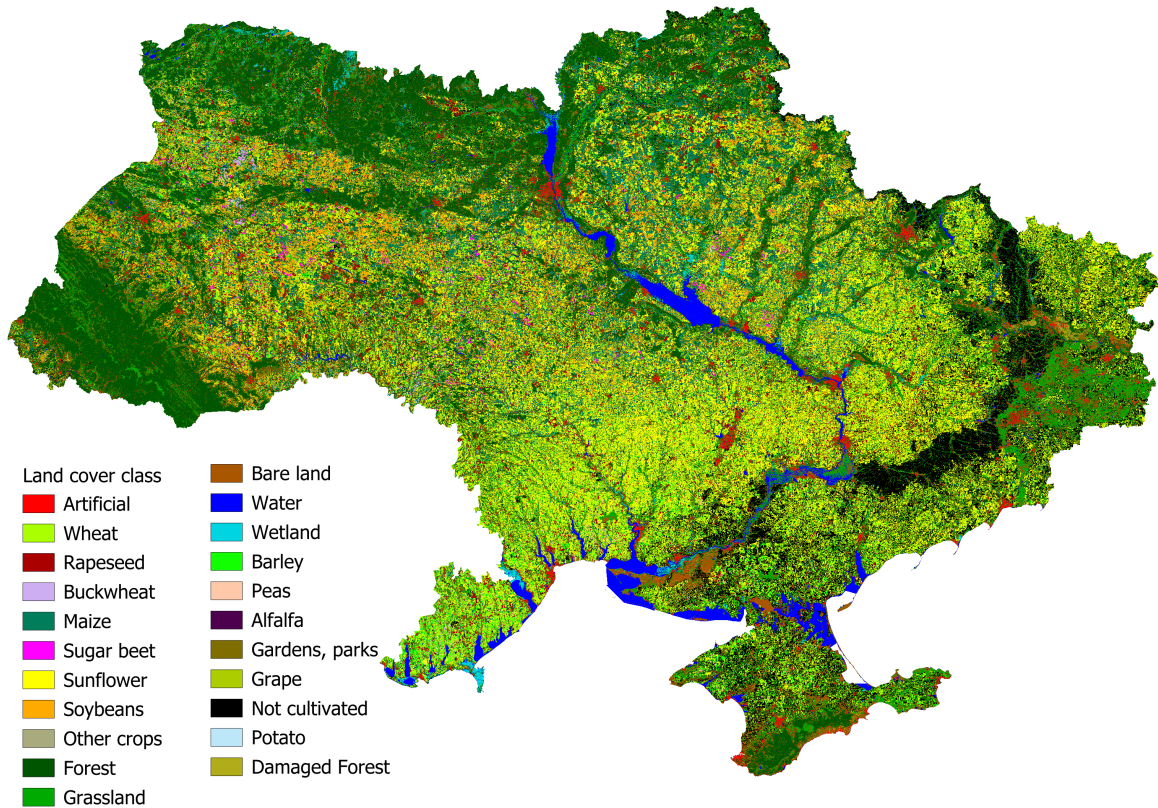


Figure 1: Land cover classification map for 2024

Table 2

F1-score and overall accuracy of land cover classification maps for Ukraine (2016-2024) [24]

	2016	2017	2018	2019	2020	2021	2022	2023	2024
Cereals		96.9	98.8	97.8					
Wheat	90.0				91.0	97.9	96.0	94.5	92.9
Barley	59.2				78.1	92.8	81.2	73.9	69.8
Rapeseed	83.6	97.0	99.1	98.9	94.3	99.2	100	97.3	99.4
Buckwheat	60.4			24.0	69.8	87.8	75.0	68.7	98.4
Maize	93.0	92.1	96.9	96.9	91.8	99.1	94.5	92.4	96.4
Sugar beet	93.6	98.6	95.5	86.6	89.4	99.4	92.9	94.5	95.0
Sunflower	94.3	95.6	98.0	98.2	93.8	99.7	98.2	98.1	98.4
Soybeans	82.5	81.6	92.3	86.9	82.4	96.2	82.2	88.7	94.4
Peas	70.9	91.8	92.9	68.6	87.7	88.5	99.5	89.5	97.4
Alfalfa				68.5	84.9	60.9	88.5	43.8	84.4
Potatoes							86.7	30.1	49.8
Grape				46.6	79.8	87.1	90.8	64.7	85.9
Gardens, parks				59.0	56.3	83.3	89.5	85.0	71.7
Other crops	34.5		66.8	34.4	19.6	72.9	16.3	71.1	20.6
Artificial	75.0	70.3	78.3	70.6	74.1	93.4	95.8	85.2	86.2
Forest	98.1	98.7	99.8	91.0	91.8	99.0	98.7	98.9	98.6
Grassland	80.2	84.3	94.7	80.5	78.0	91.1	90.0	88.3	85.7
Bare land	60.0	60.8	77.4	64.0	68.0	96.0	88.1	78.3	78.0
Water	88.6	99.2	99.0	99.2	100	100	99.8	99.7	100
Wetland	77.3	62.5	73.3	63.5	56.1	87.3	90.3	93.4	95.9
Uncultivated land								92.2	93.2
Overall accuracy	88.3	91.0	97.3	94.8	87.9	97.5	95.0	93.1	94.5



Figure 2: Example of identifying crop types on damaged fields using land cover classification: a) Damaged fields (Sentinel-2 image from 2022-07-02, coordinates: Lon: 36.238°, Lat: 47.581°); b) Land cover classification map for the area of the damaged fields.

Figure 2 shows an example of identifying crop types on damaged fields using a land cover classification map. Based on a Sentinel-2 image, damaged areas were detected [24], and according to the land cover classification map for the corresponding year, it was determined that affected fields were cultivated with wheat (class 2), rapeseed (class 3), and barley (class 15).

In general, using land cover classification maps allows:

- Identify the crop type present at the time of damage;
- Determine whether the field was abandoned in the year following the incident;
- Assess whether agricultural activity resumed after remediation efforts.

3. Identifying Periods of Land Abandonment

The previously described land cover classification maps not only help identify the types of crops present in the fields at the time of damage, but also make it possible to determine whether the field was cultivated in the following year or left fallow, and how long agricultural activities were suspended.

This is enabled by the presence of a dedicated "Not cultivated" class in the classification maps, which distinguishes abandoned land from actively farmed fields. Figure 3 illustrates this process: a field cultivated with wheat in 2022 (Figure 3a) was damaged. In both 2023 and 2024, the field was classified as abandoned (Figure 3b, c), but in 2025 it was once again cultivated – this time with wheat and buckwheat (Figure 3d). Based on this data, the 2023-2024 period can be identified as a time of abandonment.

Annual classification maps allow for such analysis at the year-to-year level. However, when more precise temporal resolution is needed – such as identifying the specific date of abandonment or the return of agricultural activity – other geospatial products may be used.

One such product is Dynamic World [25], developed by Google. It is a global near real-time land cover classification dataset, updated every 2-5 days, based on Sentinel-2 imagery and AI-driven analysis. While it offers lower accuracy and lacks specific crop type differentiation, Dynamic World can allow for the detection of land cover transitions – for instance, from cropland to grassland or shrubland, and vice versa – indicating either abandonment or re-cultivation.

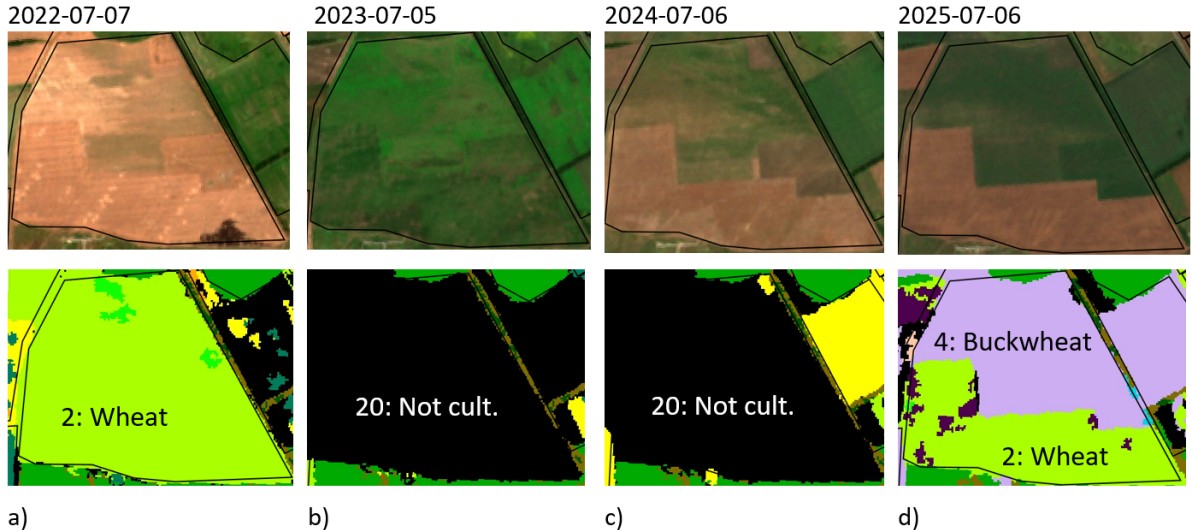


Figure 3: Example of identifying a field abandonment period using land cover classification maps (Lon: 37.111° , Lat: 49.039°). The top row shows Sentinel-2 imagery for the indicated dates, while the bottom row presents land cover classification maps for the corresponding years.

4. AI and Satellite Data Integration for Crater Detection in Damaged Fields

Satellite imagery is a powerful tool for the remote detection of damage to agricultural areas. Leveraging classical and deep machine learning methods applied to satellite data allows researchers to:

- Estimate the approximate dates of damage;
- Identify the type of damage (craters, vehicle tracks, trenches, burnt areas, etc.);
- Monitor the progression and dynamics of damage over time;
- Detect individual craters.

For most of these tasks, freely available Sentinel-2 imagery can be used [16, 17, 26]. With its high revisit frequency (every 5 days) and global coverage, Sentinel-2 enables consistent monitoring of large areas and supports the identification of damaged fields. Moreover, Sentinel-2 imagery can even be used to detect individual craters that are large enough to be visible at the 10-meter resolution. According to research findings [26] (Figure 4), Sentinel-2 images can detect approximately 51% of craters (mostly those with an area greater than 100 m^2) that were confirmed using Ultra High-Resolution Satellite Imagery (UHR), such as those provided by Maxar.

Unlike Sentinel-2, which offers frequent updates but lower spatial resolution, Maxar's WorldView satellites provide commercial imagery with a spatial resolution ranging from 0.3 to 0.5 meters. These datasets are available for selected regions and time periods, typically upon request. The high level of detail in Maxar imagery enables the detection of even very small field disturbances on specific dates.

To process these high-resolution images, it can be used deep learning models [18], particularly architectures based on U-Net (convolutional neural network), which provide accurate semantic segmentation and allow precise crater identification.

In one of the most comprehensive studies conducted by the University of Maryland [27], approximately $31,034 \text{ km}^2$ (around 5% of Ukraine's total area) was analyzed for the year 2022, focusing on regions along the front line. Craters were detected for each agricultural field (Figure 5), and the results were aggregated into a $1 \times 1 \text{ km}$ grid.

The outcome was a generalized crater density map, showing the number of craters per square kilometer across the studied area (Figure 6).

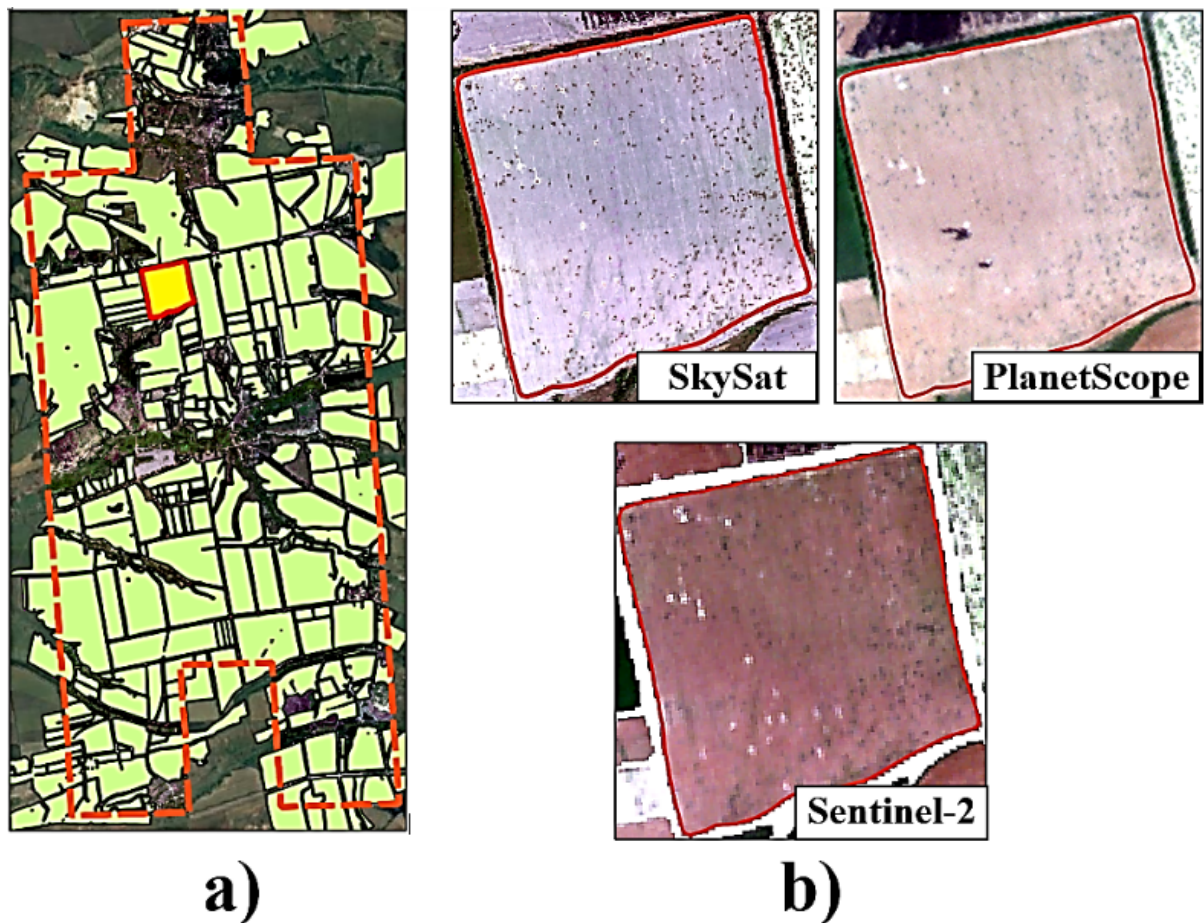


Figure 4: Example of crater appearance in imagery from three satellites with different spatial resolutions: SkySat (0.5 m), PlanetScope (3 m), and Sentinel-2 (10 m). Source: [26].

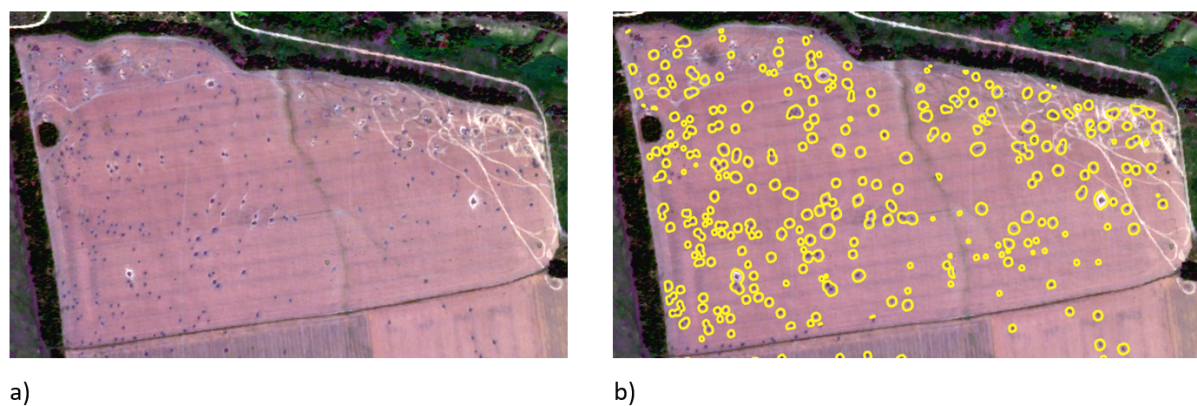


Figure 5: Example of crater detection results using Maxar imagery (2022-07-02), based on the study [18]. Coordinates: Lon: 48.66395°, Lat: 38.28779°.

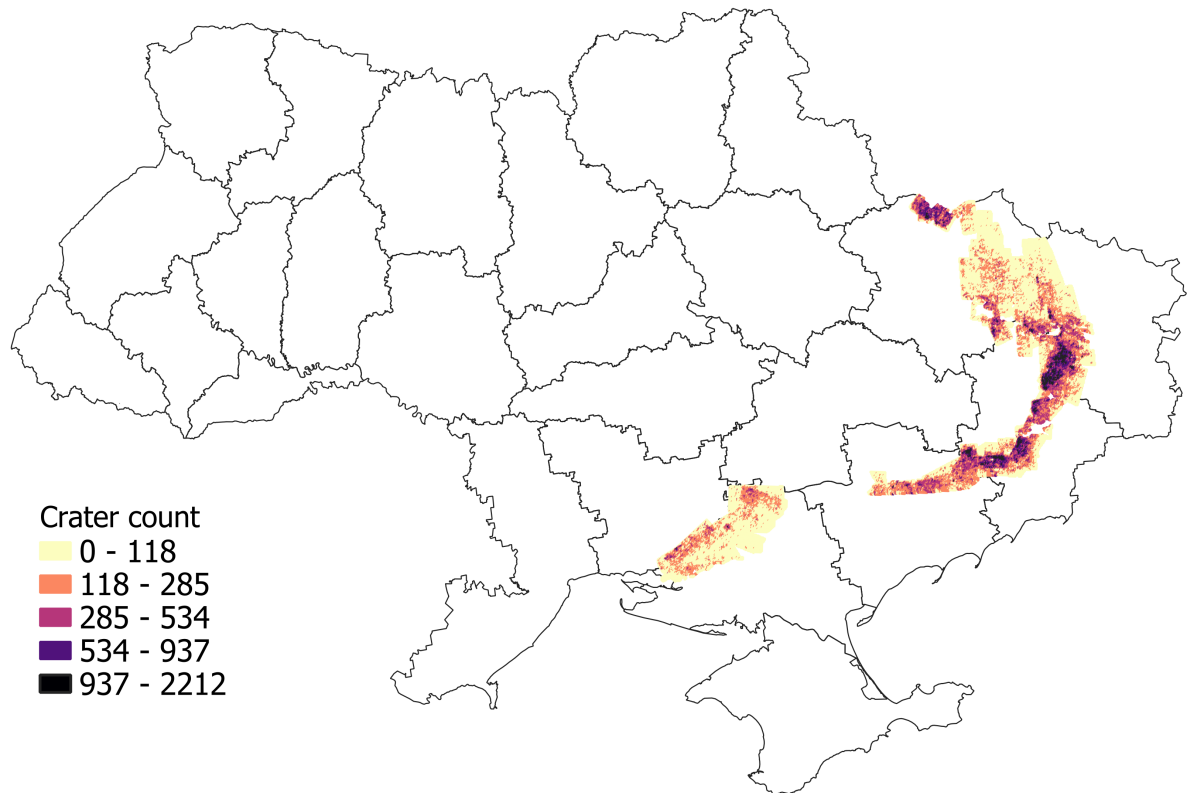


Figure 6: Crater density map (number of craters per $1 \times 1 \text{ km}^2$ grid cell) produced by the University of Maryland [27].

5. Evaluating the Impact of Demining and Remediation on Crop Yield in Conflict-Damaged Fields Using Vegetation Indices

Satellite data provide a valuable tool for assessing the effectiveness of demining and remediation measures in conflict-damaged agricultural fields. By deriving specific vegetation indices from satellite imagery, it is possible to evaluate the condition and health of vegetation [28, 29, 30], which in turn can be used to estimate land productivity and even forecast crop yields [31, 32].

One of the most widely used vegetation indices for monitoring plant health is the Normalized Difference Vegetation Index (NDVI) [33], calculated as:

$$NDVI = \frac{NIR - RED}{NIR + RED}, \quad (1)$$

where *NIR* is the reflectance in the near-infrared band, and *RED* is the reflectance in the red band. NDVI values range from -1 to 1:

- values close to -1 typically indicate water bodies or very dark surfaces;
- values near 0 usually correspond to bare soil or built-up areas;
- values approaching 1 (e.g., 0.6–0.9) represent dense, healthy vegetation.

Consequently, low NDVI values in damaged fields may indicate reduced biomass [34], poor plant condition, or incomplete recovery after damage [35]. However, in cases where fields are abandoned, invasive plant species may appear, often exhibiting high NDVI values despite not being agricultural crops. Moreover, each crop type has a distinct seasonal NDVI profile, which must be considered in the analysis.

Therefore, to assess the potential yield of damaged fields accurately, NDVI values should be extracted only from pixels corresponding to the specific crop type under investigation by applying a crop mask.

Previous studies have shown a strong positive correlation between NDVI and crop yield [36]. Depending on the availability of training yield statistics, NDVI can be used to forecast the yield of a specific crop at national, regional, or even field level. Studies have shown that, with an appropriate approach – incorporating climate data and other complementary information – yield can be predicted with relatively high accuracy several months before harvest [37].

5.1. Assessing Remediation Effectiveness through Comparative Analysis of Vegetation Dynamics in Damaged and Undamaged Fields

A damage event on a field can have a significant impact on the dynamics of vegetation indices. Figure 7 shows an example of NDVI time series for a field damaged in early June and for an adjacent undamaged field with the same crop type (wheat).

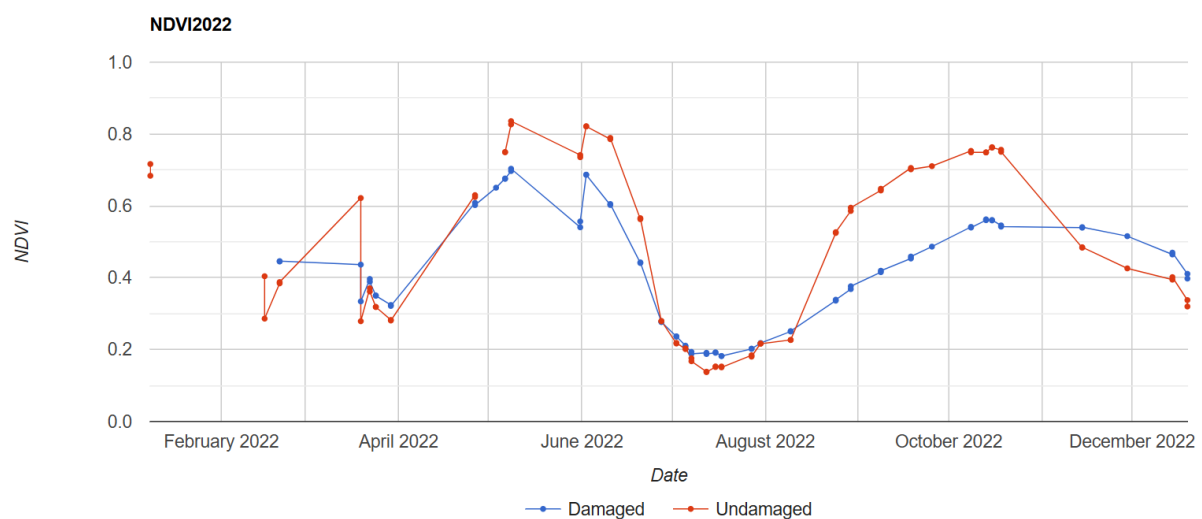


Figure 7: NDVI time series for damaged (Lon: 37.042, Lat: 49.057) and undamaged (Lon: 36.789 Lat: 48.975) fields (2022).

The graph illustrates that the undamaged field demonstrates higher NDVI values immediately after the shelling of the damaged field (June-July) as well as during the autumn period.

To further assess the impact of damage on vegetation, it is also useful to analyze NDVI dynamics for the same field across multiple years, taking into account crop classification maps.

Figure 8 presents the average monthly NDVI dynamics for a wheat field over 4 periods:

1. 2021 – before the damage;
2. 2022 – the year when the damage occurred;
3. 2024 – after partial demining and remediation measures (cultivation resumed on part of the field, Figure 8c);
4. 2025 – after complete demining and remediation measures (Figure 8c).

From the figure, it is evident that after the remediation measures and demining, the NDVI for wheat in 2024 was nearly identical to that of 2020. The decrease in NDVI observed in 2025 can be explained by two main factors: 1) as a larger portion of the field was returned to cultivation, there is a possibility that the productivity of this newly restored area remained reduced due to prior damage; 2) the changes in NDVI dynamics may have been driven simply by climatic conditions.

Analyzing a single field is not sufficient to fully assess the impact of damage and subsequent remediation measures on vegetation health. Therefore, to conduct a broader assessment, we can compare the average monthly NDVI during the 2024 growing season (April-September) for two categories of fields:

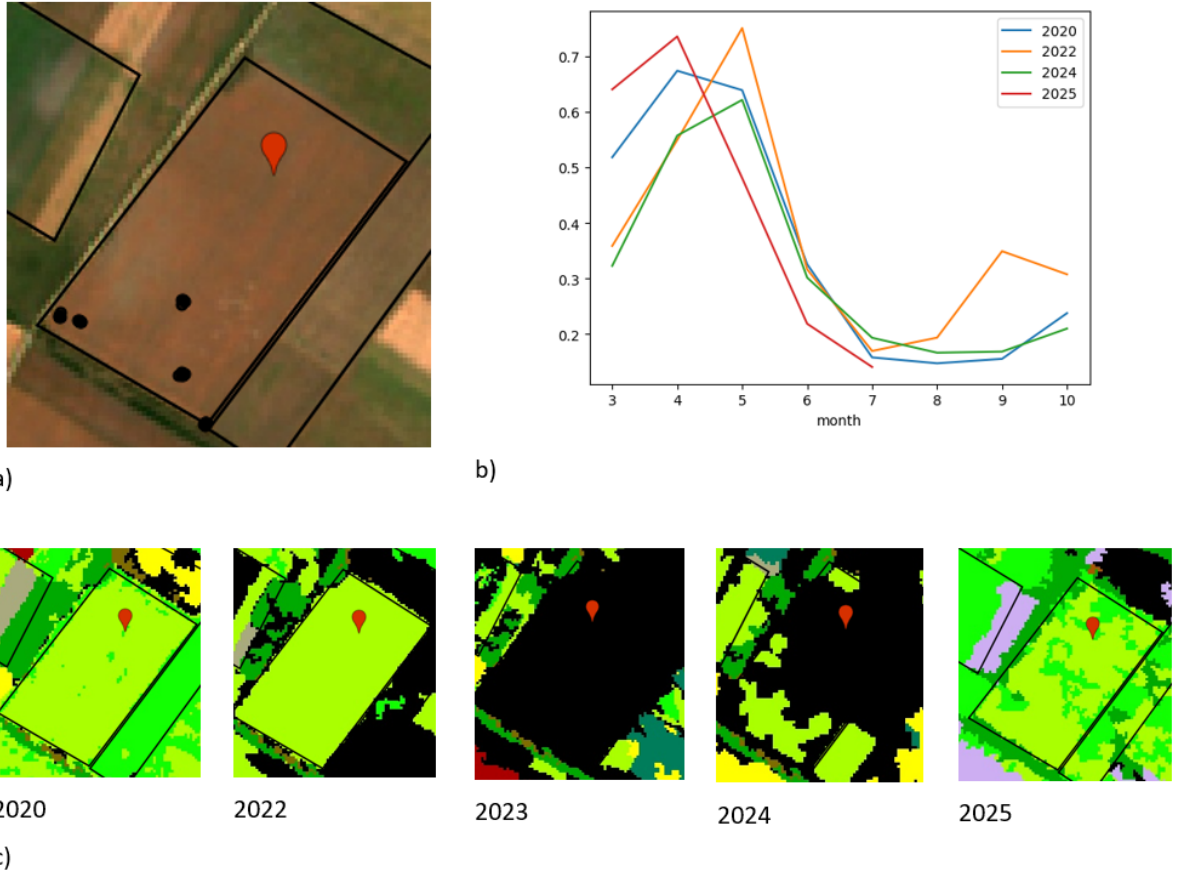


Figure 8: Example of NDVI dynamics for a wheat field before damage (2020), during damage (2022), and after demining (2024 and 2025). a) Image of the damaged field in June 2022 with identified demining points; b) Average monthly NDVI dynamics using the wheat mask; c) Land cover classification maps for the field: green indicates wheat, black indicates uncultivated land. Coordinates: Lon: 33.095, Lat: 47.063.

1. fields that had been damaged, demined, and remediated by the HALO Trust mission [8];
2. fields located in Ukrainian-controlled territory that had never been affected by shelling.

Using classification map masks for four major crops (wheat, sunflower, maize, and soybean), we examined the average NDVI for 42 fields from the first group (damaged and restored), located mainly in eastern, but also in southern and northern regions, and 47 fields from the second group (undamaged), randomly selected across southern, central, and northern Ukraine.

It should be noted that some fields in the dataset may have contained multiple crops within the same season or may have been partially or completely uncultivated. Specifically, in the first group, there were 12 fields fully or partially (number of pixels > 10) containing wheat, 9 fields with sunflower, 9 with maize, and 3 with soybean. The remaining fields contained either other crops or were uncultivated. In the second group, 15 fields contained wheat, 23 had sunflower, 15 maize, and 10 soybean.

As shown in Figure 9, for each of the studied crops, the average monthly NDVI for the first group was lower than for the second group. This difference was most pronounced for sunflower (Figure 9b) and soybean (Figure 9d). In contrast, wheat (Figure 9a) and maize (Figure 9c) fields exhibited relatively similar NDVI values in both groups.

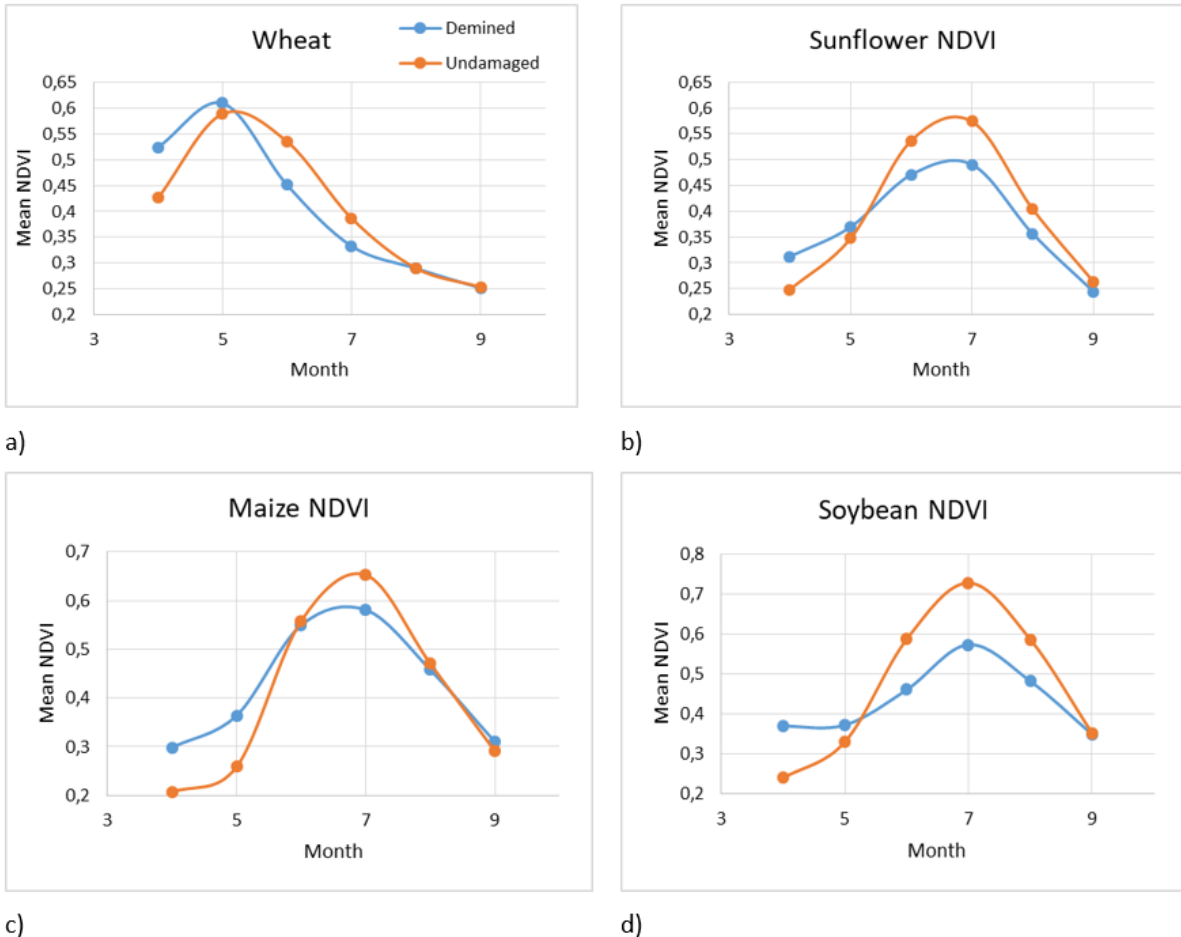


Figure 9: Average monthly NDVI (April-September 2024) for damaged fields that underwent demining and remediation, compared to undamaged fields.

6. AI-Driven Remote Sensing for Erosion Detection in War-Affected Areas

Another task that can be addressed using satellite data is the detection and monitoring of erosion processes in damaged territories.

The simplest approach to monitoring erosion is through the use of vegetation-related spectral indices. One of the most widely used is the Bare Soil Index (BSI) [38, 39], calculated as:

$$BSI = \frac{(SWIR2 + R) - (NIR + B)}{(SWIR2 + R) + (NIR + B)}, \quad (2)$$

where *SWIR2* is the reflectance in the second short-wave infrared band, *R* is the reflectance in the red band, *NIR* is the reflectance in the near-infrared band, *B* is the reflectance in the blue band, and *BSI* (Bare Soil Index) is used to highlight bare soil areas by combining these spectral bands.

The main principle is to use spectral information to identify and isolate areas of bare soil. The index separates vegetation from non-productive land and can be applied to detect landslides or assess erosion severity in non-vegetated areas. BSI values typically range from about -1 (densely vegetated) to +1 (completely bare soil). When reliable ground-based measurements of soil loss, sediment yield, or erosion depth are available, they can be combined with satellite-derived indices such as BSI to build regression models. These models can quantify the statistical relationship between remotely sensed indicators and actual erosion rates, enabling the estimation of soil loss across larger areas where direct field measurements are unavailable.

Beyond simple vegetation indices, erosion risk and intensity are often assessed using the Revised Universal Soil Loss Equation (RUSLE) [40], which estimates average annual soil loss:

$$A = R \times K \times LS \times C \times P, \quad (3)$$

where A – predicted soil loss (t/ha/year), R – rainfall erosivity factor, K – soil erodibility factor, LS – slope length and steepness factor, C – cover and management factor, P – support practice factor

Figure 10 shows the values of A , calculated using the RUSLE model [41] and satellite-derived inputs for the period 2022–2024 across the eastern part of Ukraine. In the enlarged view of a randomly selected test area, fields identified as damaged due to military activity (based on visual interpretation of satellite imagery from 2022–2024) are outlined in black. The remaining fields were not identified as damaged.

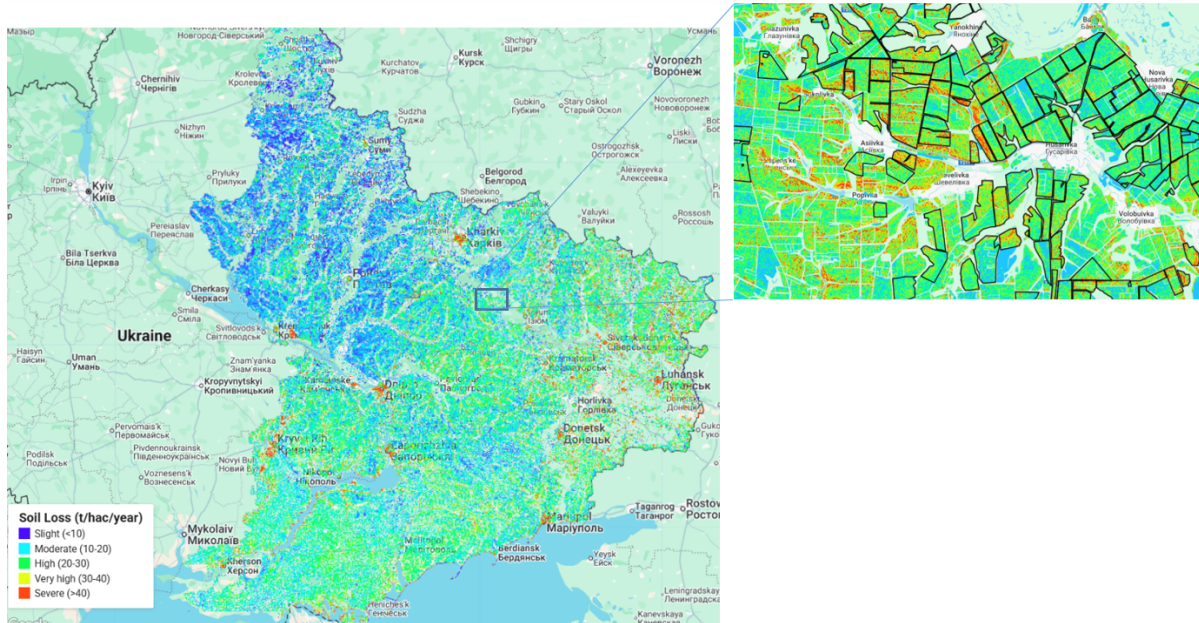


Figure 10: Soil Loss (t/ha/year) based on RUSLE model (2022-2024)

The map demonstrates that, overall, erosion risk is higher in eastern Ukraine. However, according to the RUSLE estimates, there is no clear correlation between A values and the presence of damaged fields. This indicates that erosion risk exists not only on damaged fields but also across undamaged agricultural areas, highlighting the broader need for monitoring and management.

7. Conclusion

Remote sensing technologies are an effective tool for assessing and monitoring agricultural damage caused by the ongoing conflict in Ukraine. Utilizing Sentinel-2, Maxar imagery, and advanced machine learning algorithms, satellite-based monitoring means effectively track war-related agricultural impacts from initial damage detection to long-term recovery assessment.

Annual land cover classification maps enable precise identification of affected crop types and abandonment periods, showing many fields remain uncultivated for 2-3 years following damage.

Vegetation indices analysis demonstrates significant remediation challenges. Even after comprehensive demining by organizations like the HALO Trust, damaged fields exhibit 10-20% lower NDVI values compared to undamaged areas, particularly for sunflower and soybean crops. This persistent productivity gap indicates that full agricultural recovery requires extended timeframes after initial remediation.

Additionally, RUSLE model assessments show that war damage has raised soil erosion risks across eastern Ukraine. Effective land management strategies addressing both conflict-related and environmental factors should be implemented.

The methodologies presented—combining crater detection, vegetation dynamics analysis, and erosion monitoring—provide a framework for continuous assessment of Ukraine’s agricultural recovery. These tools are essential for prioritizing remediation efforts, allocating resources effectively, and developing evidence-based reconstruction strategies. Moving forward, continued remote satellite monitoring integrated with ground-based assessments will be vital for tracking recovery and ensuring international support reaches the most critically affected areas.

Acknowledgments

The development of the methods for assessing field damage was supported by the World Bank and the European Union. Additional support was provided through NASA-funded projects, including “Assessment of the Impact of War in Ukraine on National Protected Areas”, the project under Grant 80NSSC24K0354, NASA Rapid Response Program (Grant Number 80NSSC23K1136), and NASA Harvest Program (Grant Number 80NSSC23M0032), as well as by the National Research Foundation of Ukraine project “Geospatial monitoring system for the war impact on the agriculture of Ukraine based on satellite data” (Grant Number 2023.04/0039).

Declaration on Generative AI

During the preparation of this work, the author(s) used GPT-5 Mini and Grammarly in order to: check grammar, spelling, and improve clarity. Further, the authors used GPT-5 Mini for translation. After using these tools, the authors reviewed and edited the content as needed and takes full responsibility for the publication’s content.

References

- [1] How the Russian invasion of Ukraine has further aggravated the global food crisis - consilium, 2025. URL: <https://www.consilium.europa.eu/en/infographics/how-the-russian-invasion-of-ukraine-has-further-aggravated-the-global-food-crisis/>.
- [2] P. Martyshev, M. Bogenos, O. Nivievsykyi, R. Neyter, V. Litvinov, I. Kolodazhnyi, I. Piddubnyi, E. Yurchenko, H. Stolnikovych, R. Nazarkina, AgroDigest Ukraine. January 2025, 2025. URL: https://kse.ua/AgroDigest_Ukraine_January_2025.pdf.
- [3] M. Solokha, O. Demyanyuk, L. Symochko, S. Mazur, N. Vynokurova, K. Sementsova, R. Mariychuk, Soil degradation and contamination due to armed conflict in Ukraine, Land 13 (2024) 1614.
- [4] A. Kucher, Ukrainian black soils in war: assessing the impact of hostilities on violations of the guidelines for sustainable soil management, Agricultural and Resource Economics: International Scientific E-Journal 11 (2025) 341–369.
- [5] I. Novakowska, N. Belousova, L. Hunko, Land degradation in Ukraine as a result of military operations, Acta Scientiarum Polonorum Administratio Locorum 24 (2025) 129–145.
- [6] M. Nehrey, N. Klymenko, V. Kravchenko, M. Komar, Ukrainian agriculture during the full-scale russian-ukrainian war: Consequences, policy responses and recovery strategies, Agricultural and Resource Economics: International Scientific E-Journal 11 (2025) 148–182.
- [7] A. Kovalskyi, A. Benderska, CHALLENGES IN THE MANAGEMENT OF AGRICULTURAL LAND RESOURCES DURING UKRAINE’S POST-WAR RECOVERY, Green, Blue and Digital Economy Journal 6 (2025) 45–54.
- [8] The halo trust, 2025. URL: <https://www.halotrust.org/>.
- [9] H. Kulish, Center for Food and Land Use Research (KSE Agrocenter) - Kyiv School of Economics, 2025. URL: <https://kse.ua/center-for-food-and-land-use-research-c4flure-main/>.

- [10] M. Padhiary, R. Kumar, Enhancing Agriculture Through AI vision and machine learning: the evolution of smart farming, in: *Advancements in intelligent process automation*, IGI Global, 2025, pp. 295–324.
- [11] N. Kussul, M. Lavreniuk, S. Skakun, A. Shelestov, Deep Learning Classification of Land Cover and Crop Types Using Remote Sensing Data, *IEEE Geoscience and Remote Sensing Letters* 14 (2017) 778–782. doi:10.1109/LGRS.2017.2681128.
- [12] L. Viskovic, I. N. Kosovic, T. Mastelic, Crop classification using multi-spectral and multitemporal satellite imagery with machine learning, in: *2019 International conference on software, telecommunications and computer networks (SoftCOM)*, IEEE, 2019, pp. 1–5.
- [13] G. Siesto, M. Fernández-Sellers, A. Lozano-Tello, Crop classification of satellite imagery using synthetic multitemporal and multispectral images in convolutional neural networks, *Remote Sensing* 13 (2021) 3378.
- [14] V. M. Olsen, R. Fensholt, P. Olofsson, R. Bonifacio, V. Butsic, D. Druce, D. Ray, A. V. Prishchepov, The impact of conflict-driven cropland abandonment on food insecurity in South Sudan revealed using satellite remote sensing, *Nature Food* 2 (2021) 990–996.
- [15] T. Liu, L. Yu, X. Liu, D. Peng, X. Chen, Z. Du, Y. Tu, H. Wu, Q. Zhao, A Global Review of Monitoring Cropland Abandonment Using Remote Sensing: Temporal–Spatial Patterns, Causes, Ecological Effects, and Future Prospects, *Journal of Remote Sensing* 5 (2025) 0584.
- [16] N. Kussul, S. Drozd, H. Yailymova, A. Shelestov, G. Lemoine, K. Deininger, Assessing damage to agricultural fields from military actions in Ukraine: An integrated approach using statistical indicators and machine learning, *International Journal of Applied Earth Observation and Geoinformation* 125 (2023) 103562. URL: <https://www.sciencedirect.com/science/article/pii/S1569843223003862>. doi:<https://doi.org/10.1016/j.jag.2023.103562>.
- [17] A. Shelestov, S. Drozd, P. Mikava, I. Barabash, H. Yailymova, War Damage Detection Based on Satellite Data, 2023. URL: <http://dx.doi.org/10.25673/101924>.
- [18] E. C. Duncan, S. Skakun, A. Kariyaa, A. V. Prishchepov, Detection and mapping of artillery craters with very high spatial resolution satellite imagery and deep learning, *Science of Remote Sensing* 7 (2023) 100092. URL: <https://www.sciencedirect.com/science/article/pii/S2666017223000172>. doi:<https://doi.org/10.1016/j.srs.2023.100092>.
- [19] M. Gabbrielli, M. Corti, M. Perfetto, V. Fassa, L. Bechini, Satellite-based frost damage detection in support of winter cover crops management: A case study on white mustard, *Agronomy* 12 (2022) 2025.
- [20] M. M. Islam, T. Ahamed, S. Matsushita, R. Noguchi, A damage-based crop insurance system for flash flooding: a satellite remote sensing and econometric approach, in: *Remote sensing application II: A climate change perspective in agriculture*, Springer, 2024, pp. 121–163.
- [21] S. Subedi, M. Maimaitijiang, X. Zhang, AI-assisted Large Scale Crop Damage Mapping Using Satellite Remote Sensing Data, in: *AGU Fall Meeting Abstracts*, volume 2024, 2024, pp. IN31A-07.
- [22] A. Rogachev, E. Melikhova, Monitoring of agricultural land productivity using unmanned aerial vehicles and artificial neural networks, in: *IOP Conference Series: Earth and Environmental Science*, volume 403, IOP Publishing, 2019, p. 012175.
- [23] Y. Wang, Ecological risk identification and assessment of land remediation project based on GIS technology, *Environmental Science and Pollution Research* 30 (2023) 70493–70505.
- [24] N. Kussul, A. Shelestov, B. Yailymov, H. Yailymova, G. Lemoine, K. Deininger, Assessment of war-induced agricultural land use changes in Ukraine using machine learning applied to Sentinel satellite data, *International Journal of Applied Earth Observation and Geoinformation* 140 (2025) 104551. URL: <https://www.sciencedirect.com/science/article/pii/S1569843225001980>. doi:<https://doi.org/10.1016/j.jag.2025.104551>.
- [25] C. F. Brown, S. P. Brumby, B. Guzder-Williams, T. Birch, S. B. Hyde, J. Mazzariello, W. Czerwinski, V. J. Pasquarella, R. Haertel, S. Ilyushchenko, et al., Dynamic World, Near real-time global 10 m land use land cover mapping, *Scientific data* 9 (2022) 251.
- [26] N. Kussul, S. Drozd, S. Skakun, E. Duncan, I. Becker-Reshef, Fusion of very high and moderate spatial resolution satellite data for detection and mapping of damages in agricultural fields, in: 2023

13th International Conference on Dependable Systems, Services and Technologies (DESSERT), 2023, pp. 1–7. doi:10.1109/DESSERT61349.2023.10416533.

- [27] S. Skakun, E. Duncan, I. Becker-Reshef, N. Kussul, L. Shumilo, A. Shelestov, J. Wagner, Millions of Artillery Craters in the Agricultural Fields Impact Crop Production in Ukraine Due to the Ongoing War, in: AGU Fall Meeting Abstracts, volume 2024 of *AGU Fall Meeting Abstracts*, 2024, pp. GC33O–0339.
- [28] J. Judith, R. Tamilselvi, M. P. Beham, S. Lakshmi, A. Panthakkan, S. A. Mansoori, H. A. Ahmad, Remote Sensing Based Crop Health Classification Using NDVI and Fully Connected Neural Networks, arXiv preprint arXiv:2504.10522 (2025).
- [29] F. Kogan, L. Salazar, L. Roytman, Forecasting crop production using satellite-based vegetation health indices in Kansas, USA, *International journal of remote sensing* 33 (2012) 2798–2814.
- [30] R. K. Kurbanov, N. I. Zakharova, Application of vegetation indexes to assess the condition of crops, *Agricultural Machinery and Technologies* 14 (2020) 4–11.
- [31] A. Shelestov, L. Shumilo, H. Yailymova, S. Drozd, Crop Yield Forecasting for Major Crops in Ukraine, in: 2021 IEEE International Conference on Information and Telecommunication Technologies and Radio Electronics (UkrMiCo), 2021, pp. 35–38. doi:10.1109/UkrMiCo52950.2021.9716672.
- [32] M. Ashfaq, I. Khan, R. F. Afzal, D. Shah, S. Ali, M. Tahir, Enhanced wheat yield prediction through integrated climate and satellite data using advanced AI techniques, *Scientific Reports* 15 (2025) 18093.
- [33] J. Jena, S. R. Misra, K. P. Tripathi, Normalized difference vegetation index (NDVI) and its role in agriculture, *Agriculture and Food: E-Newsletter* 1 (2019) 387–389.
- [34] J. Meng, X. Du, B. Wu, Generation of high spatial and temporal resolution NDVI and its application in crop biomass estimation, *International Journal of Digital Earth* 6 (2013) 203–218.
- [35] H. Li, J. Lei, J. Wu, Analysis of land damage and recovery process in rare earth mining area based on multi-source sequential NDVI, *Transactions of the Chinese Society of Agricultural Engineering* 34 (2018) 232–240.
- [36] E. Panek, D. Gozdowski, Analysis of relationship between cereal yield and ndvi for selected regions of central europe based on modis satellite data, *Remote Sensing Applications: Society and Environment* 17 (2020) 100286. URL: <https://www.sciencedirect.com/science/article/pii/S2352938519303027>. doi:<https://doi.org/10.1016/j.rasae.2019.100286>.
- [37] A. Barriguinha, B. Jardim, M. de Castro Neto, A. Gil, Using NDVI, climate data and machine learning to estimate yield in the Douro wine region, *International Journal of Applied Earth Observation and Geoinformation* 114 (2022) 103069. URL: <https://www.sciencedirect.com/science/article/pii/S1569843222002576>. doi:<https://doi.org/10.1016/j.jag.2022.103069>.
- [38] N. Mzid, S. Pignatti, W. Huang, R. Casa, An Analysis of Bare Soil Occurrence in Arable Croplands for Remote Sensing Topsoil Applications, *Remote Sensing* 13 (2021). URL: <https://www.mdpi.com/2072-4292/13/3/474>. doi:10.3390/rs13030474.
- [39] C. T. Nguyen, A. Chidthaisong, P. Kieu Diem, L.-Z. Huo, A Modified Soil Index to Identify Bare Land Features during Agricultural Fallow-Period in Southeast Asia Using Landsat 8, *Land* 10 (2021). URL: <https://www.mdpi.com/2073-445X/10/3/231>. doi:10.3390/land10030231.
- [40] R. Kumar, S. N. Mishra, R. Pandey, V. P. Panwar, Chapter 23 - Estimation of soil erosion risk and vulnerable zone using the revised universal soil loss equation and geographic information system approaches, in: S. Chandra Pal, U. Chatterjee, R. Chakrabortty (Eds.), *Applications of Geospatial Technology and Modeling for River Basin Management*, volume 12 of *Modern Cartography Series*, Academic Press, 2024, pp. 597–626. URL: <https://www.sciencedirect.com/science/article/pii/B9780443238901000232>. doi:<https://doi.org/10.1016/B978-0-443-23890-1.00023-2>.
- [41] Sukantjain, Rusle in gee.js, 2025. URL: <https://github.com/sukantjain/Google-Earth-Engine/blob/main/JavaScript/RUSLE%20in%20GEE.js>.